Inorganic Chemistry

pubs.acs.org/IC Article

Multi-State Dynamic Coordination Complexes Interconverted through Counterion-Controlled Phase Transfer

Ho Fung Cheng,[‡] McKinley K. Paul,[‡] Andrea I. d'Aquino, Charlotte L. Stern, and Chad A. Mirkin*

Cite This: *Inorg. Chem.* 2021, 60, 4755−4763 Read Online

ABSTRACT: We studied a series of dynamic weak-link approach (WLA) complexes that can be shuttled between two immiscible solvents and switched between two structural states via ion exchange. Here, we established that hydrophobic anions transfer cationic, amphiphilic complexes from the aqueous phase to the organic phase, while a chloride source reverses the process. As a result of the dynamic metal coordination properties of WLA complexes, the denticity of these complexes (mono- to bi-) can be modulated as they partition into different phases. In addition, we discovered that heteroligated complexes bearing ligands of different donor strengths preferentially rearrange into two homoligated complexes that are phase-partitioned to maximize the number of stronger coordination bonds. This behavior is not observed in systems with one solvent, highlighting the dynamic and stimuli-responsive nature of hemilabile ligands in a multiphasic solvent environment. Taken together, this work shows that the highly reconfigurable WLA modality can enable the design of biphasic reaction networks or chemical separations driven by straightforward salt metathesis reactions.

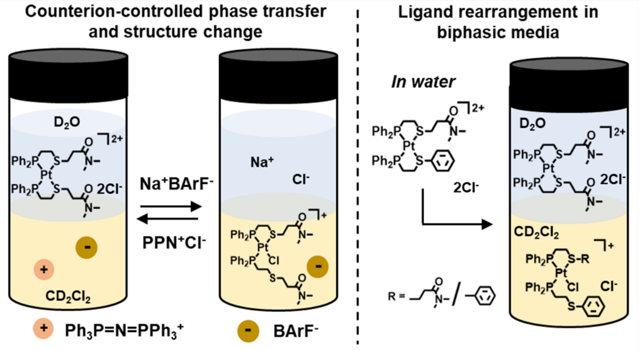

INTRODUCTION

Phase separated liquid−liquid systems are used in numerous applications due to the tailorability of solvent physical properties and solvent−substrate interactions.[1−3] Taking advantage of the heterogeneous chemical environment of liquid−liquid biphasic media, scientists have designed systems for chemical separations,[4−9] catalyst recycling,[1,10−12] and phase transfer catalysis.[13−19] For example, a selective chemical separation in a biphasic solvent medium could serve as a low energy alternative to traditional separation methods like fractional distillation. Recently, there have been demonstrations that this type of separation can be carried out by cationic coordination cages that can selectively uptake high value guest molecules.[5,9,20,21] The phase partitioning of the host−guest complex can be switched as a function of its counteranions, thus enabling extraction of a high value target molecule from its original solution. However, these coordination-based cages are static, and some must be broken down to release the encapsulated guest molecule. Taking these concepts one step further, it would be ideal if one could design complexes that could be triggered chemically to transfer phases with concomitant structural changes that either release cargo or activate the complex with respect to a desired secondary reaction.[22]

To design supramolecular architectures that exhibit dynamic conformations and stimuli-responsive reactivity as they traverse the liquid−liquid phase boundary, we first need to understand how biphasic solvent media can be used to control or even reconfigure the structure of supramolecular assemblies. We adopted the weak-link approach (WLA)[23−25] strategy to synthesize model complexes due to the dynamic nature of WLA complexes, which are typically comprised of d^8 metal centers (e.g., Pt^{II}, Pd^{II}, Rh^{I}) and multidentate, hemilabile ligands. Their overall charge, structure, and conformation can be regulated by coordination events at the metal node via elemental anions or small molecule effectors such as halides, cyanides, amines, carbon monoxide, and nitriles.[24,25] Importantly, the metal-binding affinities of halides, an important class of WLA effectors, are known to be solvent-dependent.[26] Thus, the WLA is well-suited for designing coordination complexes whose conformation changes as they undergo phase transfer.

RESULTS AND DISCUSSION

Designing Amphiphilic WLA Complexes. The dichloromethane (DCM)/water biphasic system is an attractive solvent system for several reasons: first, the polarities of water and DCM are different enough for the solvents to be immiscible but similar enough that it is feasible for a complex to be soluble

Received: December 18, 2020
Published: March 10, 2021

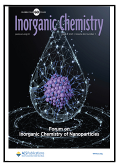

https://dx.doi.org/10.1021/acs.inorgchem.0c03708
Inorg. Chem. 2021, 60, 4755−4763

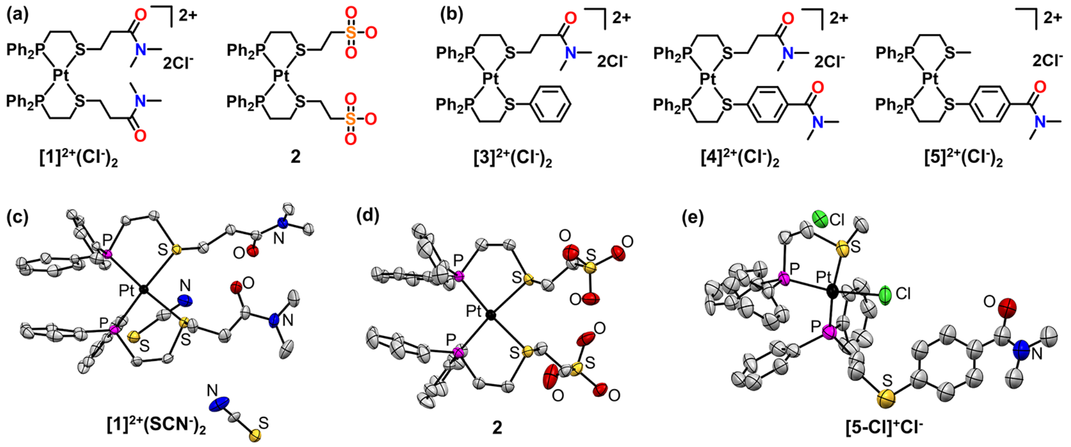

Figure 1. (a) Aqueous phase, fully closed structures of a dicationic $[\mathbf{1}]^{2+}(\mathrm{Cl}^-)_2$ and a neutral [**2**] homoligated WLA complex. (b) Aqueous phase, fully closed structures of the heteroligated WLA complexes investigated in this work. Each complex represents a unique placement of the water-solubilizing dimethyl amide moiety. Crystal structures (50% probability ellipsoids) of (c) $\mathrm{Pt(SCN)_2(P,S\text{-}ethyl\text{-}CONMe_2)_2}$ $[\mathbf{1}]^{2+}(\mathrm{SCN}^-)_2$, (d) $\mathrm{Pt(P,S\text{-}ethyl\text{-}SO_3)_2}$ [**2**], and (e) $\mathrm{PtCl_2(P,S\text{-}Me)(P,S\text{-}Ph{-}CONMe_2)}$ $[\mathbf{5}\text{-Cl}]^{+}\mathrm{Cl}^-$. Hydrogen atoms and solvent molecules are omitted for clarity.

in both solvents. Second, both solvents are readily available in deuterated forms, allowing for the characterization of the WLA complexes via nuclear magnetic resonance (NMR) spectroscopy. Finally, water is a green solvent, and introducing water solubility to WLA complexes opens the door to designing systems that incorporate complex and functional biomolecules. WLA complexes are known to be soluble in various organic solvents, but there is only one reported example of a water-soluble WLA complex,[27] which had polyethylene glycol units appended onto its highly hydrophobic diphenylphosphino moieties. As such, we set out to design and synthesize a family of amphiphilic WLA complexes that are soluble in both organic solvents and water, ideally without any extensive modification of pendant functional groups. Inspired by our initial observation that WLA complexes with mostly hydrophobic ligands can be solubilized in partially aqueous solvents, we reasoned that a simple installation of a polar functional group could be a sufficient nudge to fully solubilize the complexes in water.

To test this hypothesis, we synthesized a $\mathrm{Pt^{II}}$ complex with two hemilabile phosphino thioether (P,S) ligands, each with an ethylene dimethyl amide ($\mathrm{-CH_2CH_2-CONMe_2}$) attached to the weak-link thioether substituent (Figure 1a). Indeed, the homoligated complex $\mathrm{PtCl_2(P,S\text{-}ethyl\text{-}CONMe_2)_2}$ $[\mathbf{1}]^{2+}(\mathrm{Cl}^-)_2$ is soluble in both DCM and water but adopts different structural states in each solvent (*vide infra*). Single crystal X-ray diffraction (SCXRD) studies of the anion-exchanged complex $[\mathbf{1}]^{2+}(\mathrm{SCN}^-)_2$ confirmed the incorporation of $\mathrm{-CONMe_2}$ as part of the ligand architecture, as well as its fully closed, bidentate structural state (Figure 1c). Water solubility is attributed to the polar and hydrogen bond participating amide groups as well as the high solvation energy of the chloride counterions in water.

Encouraged by this observation, we synthesized a series of homoligated WLA complexes with P,S ligands installed with different polar functional groups such as phenyl dimethylamide ($\mathrm{PtCl_2(P,S\text{-}phenyl\text{-}CONMe_2)_2}$), amines ($\mathrm{PtCl_2(P,S\text{-}phenyl\text{-}NH_2)_2}$), carboxylic acids ($\mathrm{PtCl_2(P,S\text{-}phenyl\text{-}CO_2H)_2}$), and sulfonates ($\mathrm{Pt(P,S\text{-}ethyl\text{-}SO_3)_2}$) [**2**] (see SI Section 1), all of which were found to be soluble in water to varying degrees. Of note is the neutral homoligated complex [**2**] (Figure 1a), consisting of two anionic $\mathrm{P,S\text{-}ethyl\text{-}SO_3^-}$ ligands. This structure is important for investigating the effect of charge on mediating phase transfer. SCXRD studies confirmed the incorporation of sulfonate functional groups, the lack of any outersphere counterions, and the fully closed structural state (Figure 1d). As such, the highly hydrophilic sulfonate moieties render the complex soluble in water but insoluble in non-hydrogen-bonding organic solvents such as DCM.

We then proceeded to investigate the water solubility of a series of heteroligated complexes (Figure 1b). To study the impact of ligand electronics on the conformation and reactivity of heteroligated complexes in a biphasic solvent medium, we intentionally functionalized them with a dimethyl amide moiety at different locations: at an electron-donating alkyl thioether, at an electron-withdrawing phenyl thioether, or at both thioether substituents, all of which resulted in water-soluble complexes. The heteroligated structure of the semi-open complex $[\mathbf{5}\text{-Cl}]^{+}\mathrm{Cl}^-$ was confirmed by SCXRD (Figure 1e). All of the homoligated and heteroligated WLA complexes studied adopt the fully closed state in water, as it is energetically more favorable for both chlorides to be solvated than to form the Pt−Cl bond required to form any of the open states.[26] On the other hand, in a less polar solvent such as DCM, chloride is less well solvated and has a higher propensity to bind to the $\mathrm{Pt^{II}}$ node, yielding semi-open WLA complexes in general.

An important feature of many WLA complexes is that they are charge-balanced by counteranions. When sodium iodide or sodium thiocyanate was added to an aqueous solution of complex $[\mathbf{1}]^{2+}(\mathrm{Cl}^-)_2$, a precipitate immediately formed, indicating that hydrophilic counteranions are crucial for solubilizing these cationic complexes in water. This observation led us to hypothesize that, by using ions of different sizes and hydrophobicity, one would be able to shuttle an amphiphilic WLA complex between two immiscible solvents of different polarities in a biphasic system. Furthermore, if the effectors employed are well solvated in the aqueous phase but poorly solvated in the organic phase, the complex could exhibit a solvent-modulated conformational change due to the solvent dependent binding affinities of the effectors.[26]

Phase Transfer of a Dicationic Complex via Anion Exchange. Throughout the phase transfer experiments, $^{31}\mathrm{P}\{^{1}\mathrm{H}\}$ NMR spectroscopy was employed as the major

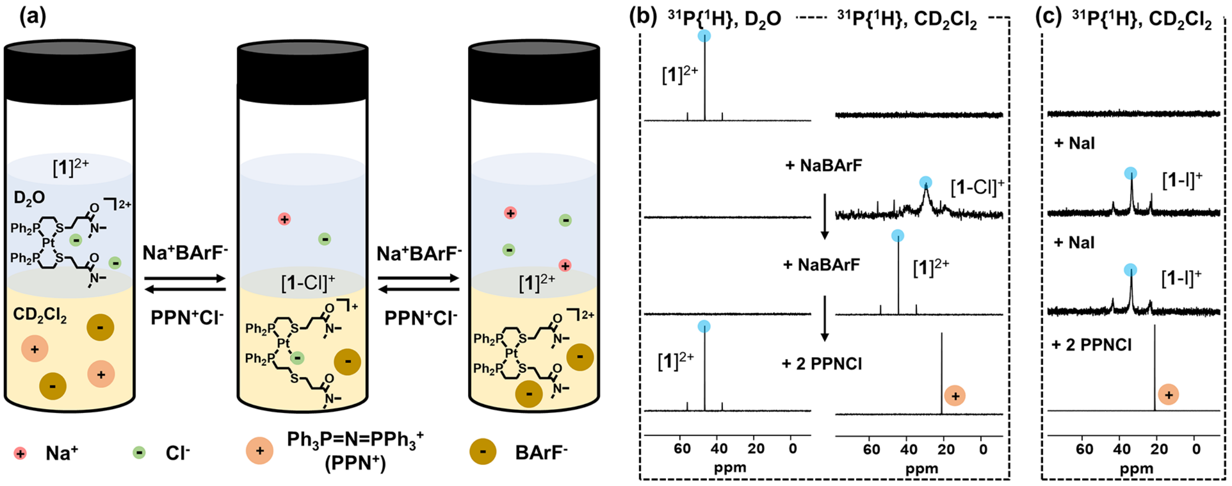

Figure 2. (a) The influence of counteranions on the partitioning and structure of the fully closed complex $[\mathbf{1}]^{2+}$ via the action of $BArF^-$ (forward direction) and PPN^+ (reverse direction). The $^{31}P\{^1H\}$ NMR spectra of complex $[\mathbf{1}]^{2+}$ upon anion exchange with (b) NaBArF and (c) NaI (see Figure S31 for the D_2O spectra) and later after the addition of PPN^+Cl^-. Blue dots track the metal complex across both phases.

characterization tool for WLA complexes owing to its high sensitivity to the ligand chemical environment and its ability to probe *in situ*, solution-state structures.[28,29]

When placed in a CD_2Cl_2/D_2O biphasic system, $PtCl_2$(P,S-ethyl-$CONMe_2$)$_2$ $[\mathbf{1}]^{2+}(Cl^-)_2$ fully partitioned into water as a fully closed, dicationic complex with two outer sphere chlorides (Figure 2a). The $^{31}P\{^1H\}$ NMR spectrum of the CD_2Cl_2 layer showed no signal (Figure 2b), while that of the D_2O layer revealed a downfield singlet (δ_P 46.49, $^1J_{P-Pt}$ = 3056 Hz), characteristic of a ^{31}P nuclei in a fully chelated (κ^2) state. We hypothesized that the salt metathesis between $[\mathbf{1}]^{2+}(Cl^-)_2$ and sodium tetrakis[3,5-bis(trifluoromethyl)phenyl]borate (NaBArF) would transfer the complex to DCM, leaving sodium chloride in the aqueous phase. When one equivalent of NaBArF was added, the $^{31}P\{^1H\}$ signal in the D_2O layer disappeared (Figure 2b), while a broad upfield signal (δ_P 29.30, $^1J_{P-Pt}$ = 3330 Hz) emerged in the CD_2Cl_2 layer. The appearance of a broad signal is characteristic of a conformationally dynamic complex undergoing rapid ligand exchange at its inner coordination sphere. Specifically, a fast "windshield wiper" exchange occurs between the two equivalent semi-open structures of $[\mathbf{1}\text{-Cl}]^+$ $BArF^-$ in DCM,[30,31] where the halide alternately cleaves each ligands' Pt^{II}–S bond.

After a second equivalent of NaBArF was added, complex $[\mathbf{1}]^{2+}$ was charge-balanced by two non-coordinating $BArF^-$ anions and switched back to the fully closed state in the CD_2Cl_2 layer as evidenced by $^{31}P\{^1H\}$ NMR spectroscopy (δ_P 44.28, $^1J_{P-Pt}$ = 3104 Hz; Figure 2b) and MALDI-TOF MS (matrix-assisted laser desorption ionization time-of-flight mass spectra) (Figure S40). Importantly, when sodium salts with smaller and less hydrophobic non-coordinating counteranions were added, such as tetrafluoroborate (BF_4^-) and hexafluoroantimonate (SbF_6^-), no phase transfer was observed, and the fully closed complex $[\mathbf{1}]^{2+}$ was completely retained in the aqueous phase (Figure S30). Alternatively, when one equivalent of sodium tetraphenylborate ($NaBPh_4$) was added, the metal complex only partly partitioned into DCM as $[\mathbf{1}\text{-Cl}]^+$ BPh_4^- (Figure S32) due to the smaller size and higher charge density of BPh_4^- compared to that of $BArF^-$. Complete transfer into DCM as $[\mathbf{1}]^{2+}$ $(BPh_4^-)_2$ was achieved using two equivalents of $NaBPh_4$. These results demonstrate that counterion size and hydrophobicity control the phase partitioning of charged amphiphilic WLA complexes.

Because DCM is a less polar solvent that favors the semi-open state, we hypothesized that a large coordinating anion such as iodide could readily mediate phase transfer, even though I^- is smaller than SbF_6^- and similar in size to BF_4^-.[32] When one equivalent of sodium iodide (NaI) was added, the $^{31}P\{^1H\}$ signal in the D_2O layer disappeared (Figure S31), while a broad upfield signal (δ_P 33.36, $^1J_{P-Pt}$ = 3220 Hz; Figure 2c) emerged in the CD_2Cl_2 layer. The slightly upfield $^{31}P\{^1H\}$ signal and smaller coupling constant, compared to that of $[\mathbf{1}\text{-Cl}]^+$ $BArF^-$ (δ_P 29.30, $^1J_{P-Pt}$ = 3330 Hz), indicates that chloride is not coordinating to the Pt^{2+} node of this complex. Moreover, the $^{31}P\{^1H\}$ NMR spectra of the CD_2Cl_2 layer are identical after the first and second anion exchange. This, together with MALDI-TOF MS (Figure S39), suggests that iodide preferentially functions as an inner sphere ligand at the Pt^{2+} node, resulting in a charge-diffuse, semi-open complex $[\mathbf{1}\text{-I}]^+$ that is partitioned into the organic phase.

To reverse these transformations, we hypothesized that a chloride salt with a large cation would enable a salt metathesis reaction that pairs the more hydrophobic counterions and reassociates $[\mathbf{1}]^{2+}$ with chlorides. Thus, $[\mathbf{1}]^{2+}(X^-)_2$ (X^- = I^-, $BArF^-$) was treated with two equivalents of bis(triphenylphosphoranylidene) ammonium chloride (PPN^+Cl^-). $^{31}P\{^1H\}$ NMR spectra of the two phases confirmed our hypothesis—the hydrophobic, charge-diffuse counterions (PPN^+ and $BArF^-/I^-$) partitioned into DCM, and $[\mathbf{1}]^{2+}$ was sent back to the aqueous phase in the fully closed state (δ_P 46.56, $^1J_{P-Pt}$ = 3060 Hz; Figure 2b and 2c). Importantly, this is achieved by designing for the mismatched solvation preference between the ions: PPN^+ prefers the organic phase, while Cl^- prefers the aqueous phase. To balance the charge, the least hydrophobic cation, $[\mathbf{1}]^{2+}$, would be forced to partition into the aqueous phase along with Cl^-.

Overall, this sequence of transformations shows that WLA complexes can be reversibly transferred between two immiscible phases via anion exchange (Figure 2). By leveraging the hemilabile nature of a multidentate ligand, phase transfer can be coupled to a metal complex's ligand conformation and dynamics, depending on the choice of counteranions. In a

https://dx.doi.org/10.1021/acs.inorgchem.0c03708
Inorg. Chem. 2021, 60, 4755–4763

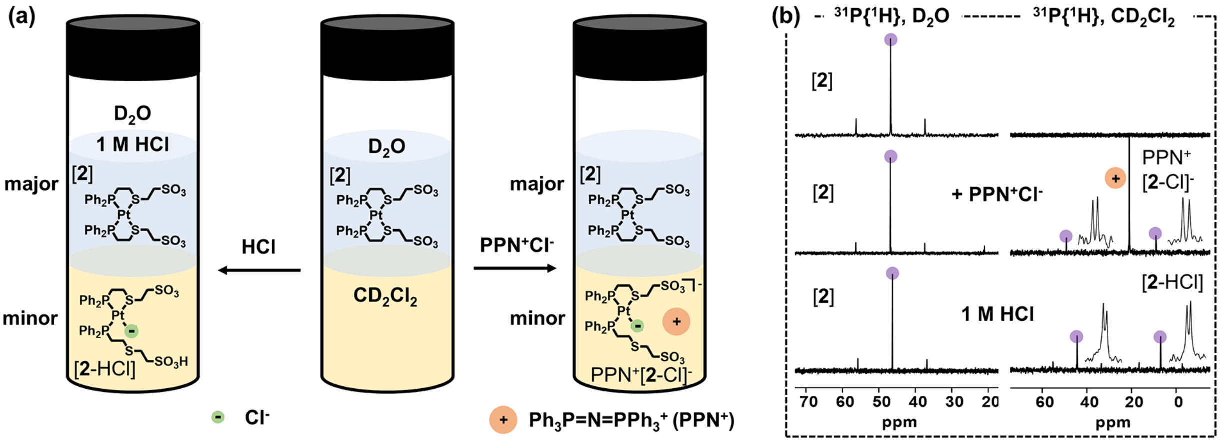

Figure 3. (a) Only a small fraction of the fully closed neutral complex [**2**] with no counteranions undergoes phase transfer in the presence of PPN$^+$Cl$^-$ (right vial) or at low pH (left vial). (b) ^{31}P{^{1}H} NMR spectra of complex [**2**] and after the addition of one equivalent of PPN$^+$Cl$^-$ and HCl. Purple dots track the metal complex across both phases. Inserts magnify the doublet features.

biphasic medium, chloride serves to "close" these metal complexes, which represents a paradigm shift from the previous notion that chloride functions as an effector that "opens" WLA complexes.

Phase Transfer of a Neutral Complex. If ion exchange indeed drives phase transfer, a charge-neutral complex should not partition into a different phase upon the addition of salts with large counterions. To test this hypothesis, we synthesized and studied the homoligated complex Pt(P,S-ethyl-SO$_3$)$_2$ [**2**], as it is highly polar, soluble in water, and charge neutral—two sulfonate groups balance the dicationic charge of Pt^{2+}. Like complex [**1**]$^{2+}$(Cl$^-$)$_2$, Pt(P,S-ethyl-SO$_3$)$_2$ [**2**] partitions into water in the biphasic system as a fully closed structure (Figure 3a). The ^{31}P{^{1}H} NMR spectrum of the CD$_2$Cl$_2$ layer showed no signal (Figure 3b), while that of the D$_2$O layer revealed a downfield singlet (δ_p 46.80, $^1J_{P-Pt}$ = 3059 Hz). When one equivalent of PPN$^+$Cl$^-$ was added, the ^{31}P{^{1}H} NMR spectrum revealed qualitatively that only a small fraction of complex [**2**] partitioned into DCM as a semi-open complex (δ_p 49.14, $^3J_{P-P}$ = 17.4 Hz and δ_p 9.03, $^3J_{P-P}$ = 17.4 Hz; Figure 3b). The phase transfer of the chloride adduct [**2**-Cl]$^-$ is presumably aided by ion-pairing with the charge-diffuse countercation PPN$^+$ (δ_p 20.99), as no phase transfer can be detected if sodium chloride was added instead of PPN$^+$Cl$^-$. On a similar note, no phase transfer was observed upon the addition of excess NaI (five equivalents) to complex **2** (Figure S33). These observations suggest that, compared to neutral complexes, charged metal complexes are more suited for enabling switchable phase transfer capabilities.

We then questioned whether we could trigger the transformation of complex [**2**] to a positively charged state by protonating a sulfonate moiety, such that complex [**2**] could be transferred to DCM by association with an anion. When the experiment was performed with 1 M hydrochloric acid and DCM, a small fraction of the fully closed complex [**2**] partitioned into DCM by forming semi-open [**2**-HCl]. The ^{31}P{^{1}H} NMR spectrum of the CD$_2$Cl$_2$ layer (Figure 3b) showed two doublets (δ_p 44.32, $^1J_{P-Pt}$ = 3503 Hz, $^3J_{P-P}$ = 15.3 Hz; and δ_p 6.93, $^1J_{P-Pt}$ = 3128 Hz, $^3J_{P-P}$ = 15.6 Hz), indicative of a semi-open complex with two nonequivalent ^{31}P nuclei. The downfield doublet was assigned to the chelating (κ^2) P,S ligand, while the upfield doublet was assigned to the nonchelating (κ^1) phosphine-bound ligand.[29,30,33] We hypothesized that some of the anionic sulfonate moieties became protonated and, as a result, a small fraction of monocationic complex [**2**-H]$^+$ was formed. Upon chloride coordination, the charge neutral [**2**-HCl] partitioned into DCM, adopting the semi-open state.

Experiments with complex [**2**] highlight the importance of considering the overall charge when designing WLA complexes for multiphasic systems. In the future, WLA complexes whose overall charge is switchable by external stimuli (e.g., pH) could be used to regulate WLA complex conformation and phase partitioning.

Selective Phase Transfer of Homoligated Complexes via Cation Exchange. So far, we have shown that anion exchange can mediate the phase transfer of a WLA complex in a biphasic medium. To investigate if cation exchange can be utilized to mediate phase transfer of an anionic metal complex, we studied the reaction between WLA complexes and cyanide anions (CN$^-$).[34]

Specifically, we added one equivalent of potassium cyanide (KCN) to complexes [**1**]$^{2+}$(Cl$^-$)$_2$ (Figure 4) and [**2**] (Figure 5), respectively. The addition of KCN to an aqueous solution

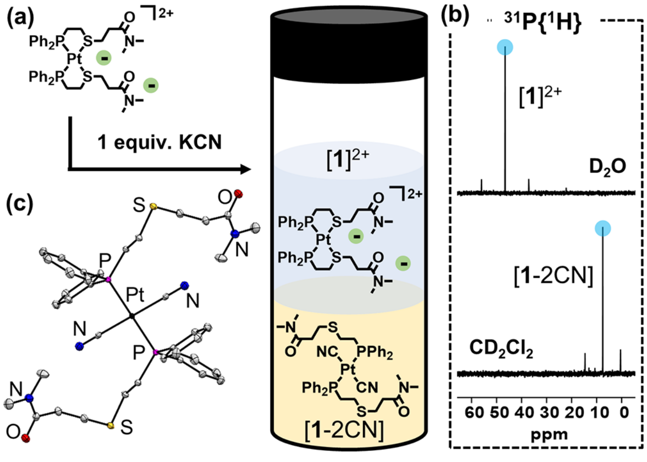

Figure 4. (a) Reaction of the fully closed complex [**1**]$^{2+}$(Cl$^-$)$_2$ with KCN in biphasic condition. (b) ^{31}P{^{1}H} NMR spectra after the reaction with KCN. (c) Crystal structure (drawn with 50% probability ellipsoids) of the fully open [**1**-2CN].

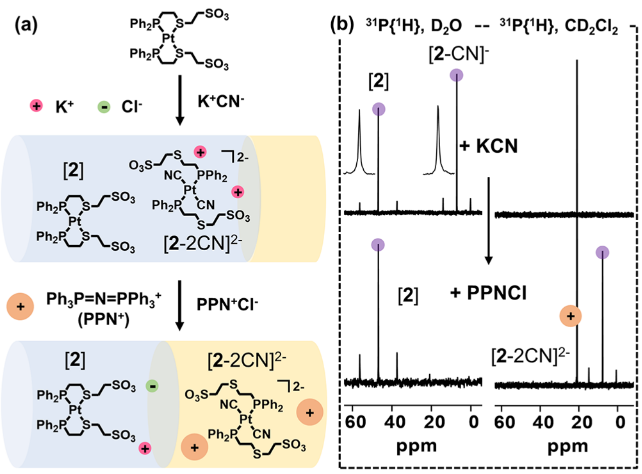

Figure 5. (a) The fully closed complex [2] reacted with KCN in biphasic condition (top), and selective partitioning of the charged species occurred via cation exchange (bottom). (b) $^{31}P\{^1H\}$ NMR spectra before and after the addition of PPN^+Cl^-. Purple dots track the metal complex across both phases. Inserts show singlet instead of doublet features upon addition of KCN.

of the fully closed $[\mathbf{1}]^{2+}(Cl^-)_2$ gave a suspension that cleared after the addition of CD_2Cl_2. The $^{31}P\{^1H\}$ NMR spectrum of the CD_2Cl_2 layer revealed an upfield signal (δ_p 7.54, $^1J_{P-Pt}$ = 2298 Hz) indicative of the fully open complex [**1**-2CN], while that of the D_2O layer showed a downfield signal (δ_p 46.58, $^1J_{P-Pt}$ = 3059 Hz), corresponding to the fully closed complex $[\mathbf{1}]^{2+}$ (Figure 4b). The NMR assignments are consistent with MALDI-TOF MS characterization (Figures S41 and S42). In particular, the small coupling constant ($^1J_{P-Pt}$ = 2298 Hz) indicates that the ^{31}P nuclei are *trans* to a strongly coordinating ligand. To study the structure of [**1**-2CN], diethyl ether was slowly diffused into the DCM layer, resulting in the formation of colorless crystals. SCXRD revealed that [**1**-2CN] adopts a *trans* configuration (Figure 4c) due to cyanides' large *trans* effect.[34−37] The differential partitioning observed here can be understood on the basis of charge and polarity.

On the contrary, when one equivalent of KCN was added to the charge-neutral, fully closed complex [**2**] in water, no precipitate formed. The $^{31}P\{^1H\}$ NMR spectrum (Figure 5b) revealed a downfield (δ_p 46.85, $^1J_{P-Pt}$ = 3057 Hz) and upfield singlet (δ_p 7.13, $^1J_{P-Pt}$ = 2250 Hz), corresponding to the fully closed complex [**2**] and the fully open complex $(K^+)_2[\mathbf{2}\text{-}2CN]^{2-}$, respectively. The small coupling constant ($^1J_{P-Pt}$ = 2250 Hz) indicates that the latter adopts a *trans* configuration. In a biphasic medium, both partition into the aqueous phase (Figure 5b). We hypothesized that the addition of PPN^+Cl^- would lead to the selective phase transfer of the charged, fully open complex to DCM via cation exchange. Satisfyingly, the $^{31}P\{^1H\}$ NMR spectrum (Figure 5b) revealed that the fully open $(PPN^+)_2[\mathbf{2}\text{-}2CN]^{2-}$ (δ_p 7.74, $^1J_{P-Pt}$ = 2294 Hz) partitioned into DCM, while the fully closed, charge-neutral complex [**2**] (δ_p 46.86, $^1J_{P-Pt}$ = 3060 Hz) remained in water. This confirms that the ion exchange mechanism is general (both cation and anion exchange can mediate phase transfer) and can operate selectively on metal complexes with an overall charge.

Heteroligated Complexes in a Biphasic Medium. A wide variety of functional metallo-supramolecular constructs have been built upon heteroligated WLA scaffolds.[38−40] Thus, it is important to study the stability and reactivity of heteroligated structures in a biphasic system. To this end, a series of heteroligated WLA complexes with varying weak-link donor strengths and ligand polarities was prepared (Figure 1b). We systematically varied the placement of the polar dimethyl amide moiety, installing it at the more donating thioether ligand ($[\mathbf{3}]^{2+}(Cl^-)_2$), at the less donating thioether ligand ($[\mathbf{5}]^{2+}(Cl^-)_2$), or at both ligands ($[\mathbf{4}]^{2+}(Cl^-)_2$).

When $PtCl_2$(P,S-ethyl-$CONMe_2$)(P,S-phenyl) $[\mathbf{3}]^{2+}(Cl^-)_2$ was dissolved in CD_2Cl_2/D_2O, the $^{31}P\{^1H\}$ NMR spectrum (Figure 6a) revealed, to our surprise, a singlet (δ_p 46.50, $^1J_{P-Pt}$ = 3059 Hz) in the D_2O layer that grew in intensity over time, indicating the gradual formation of the homoligated, fully closed complex $PtCl_2$(P,S-ethyl-$CONMe_2)_2$ $[\mathbf{1}]^{2+}$. At equilibrium, reached after 3 days, only a small fraction of the starting fully closed complex $[\mathbf{3}]^{2+}$ was present in the D_2O layer. MADLI-TOF MS confirmed that the homoligated complex $PtCl_2$(P,S-phenyl$)_2$ was present in DCM, while complex $[\mathbf{1}]^{2+}(Cl^-)_2$ was only detected in water (Figures S32 and S33). Crucially, no rearrangement was observed over one week when the heteroligated complexes are simply dissolved in water (Figure S34).

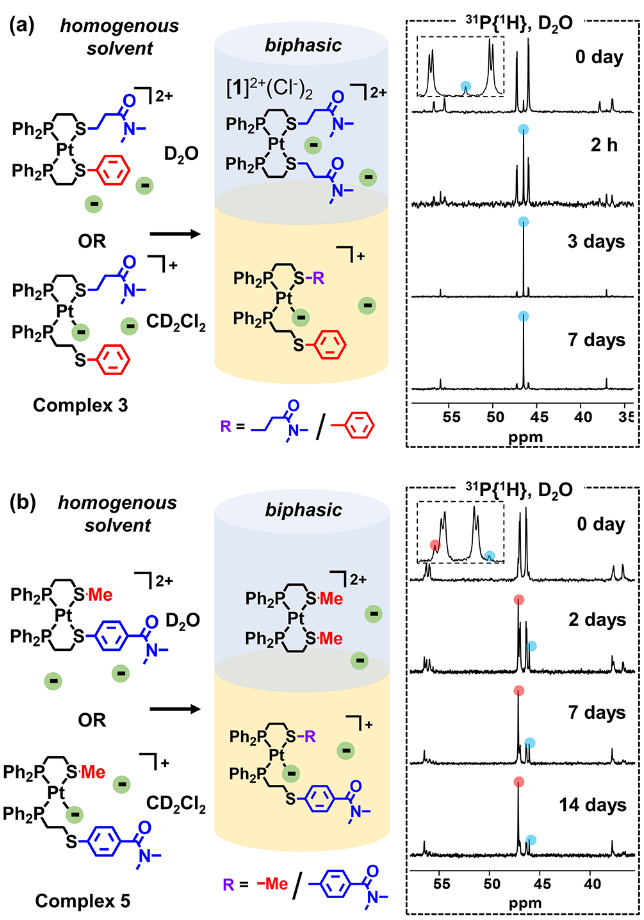

Figure 6. Major species formed after ligand rearrangement of heteroligated complexes (a) $[\mathbf{3}]^{2+}(Cl^-)_2$ and (b) $[\mathbf{5}]^{2+}(Cl^-)_2$ in D_2O/CD_2Cl_2 (left) and the $^{31}P\{^1H\}$ NMR spectra of the D_2O layers as a function of time (right). Homoligated complexes with polar (blue dots) or nonpolar (red dots) ligands. Inserts magnify the doublet features.

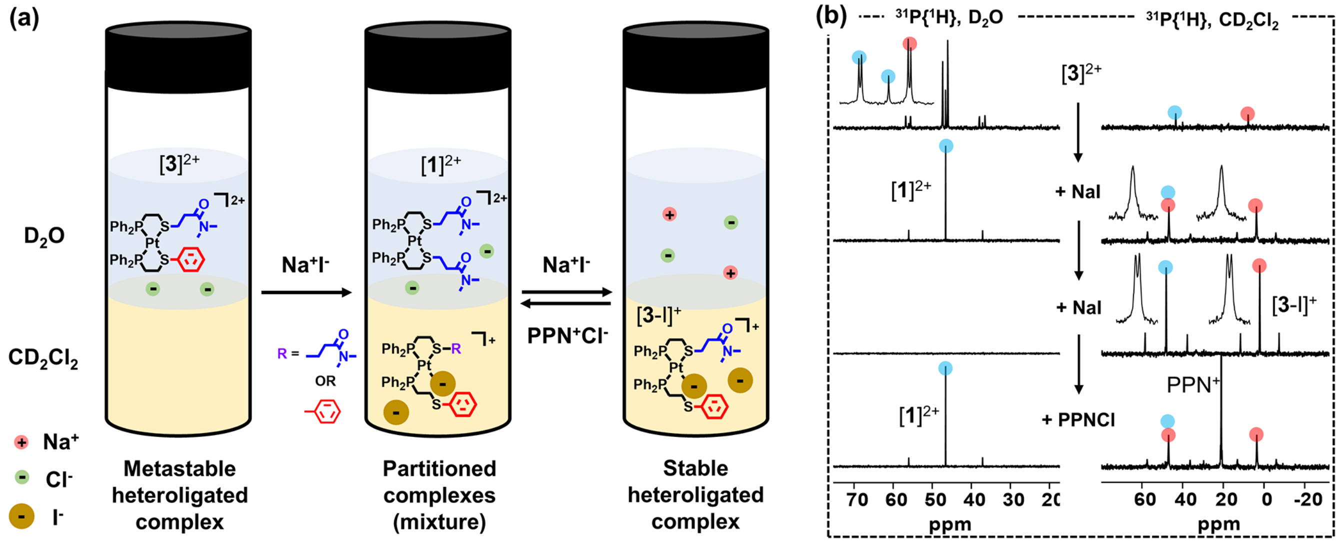

Figure 7. (a) Counteranion-mediated hemilabile ligand rearrangement of the heteroligated, fully closed complex $[\mathbf{3}]^{2+}(\mathrm{Cl}^-)_2$ from a metastable state (left vial) to a phase-separated mixture (middle vial) and a stable heteroligated, semi-open complex (right vial). (b) ^{31}P{^{1}H} NMR spectra upon sequential addition of NaI and PPN$^+$Cl$^-$. Blue dots track polar ligand while red dots track nonpolar ligand across both phases. Inserts show the doublet features or broad peaks.

The rearrangement of a heteroligated complex into two homoligated species is opposite of what has been previously observed in WLA systems.[30,41−43] In DCM, two different homoligated species with chloride counterions will typically reconfigure into one heteroligated complex if the two ligands involved possess weak links with sufficiently different donating strength.[31] Key to this halide-induced ligand rearrangement (HILR) mechanism is that, in DCM, halides are able to reversibly displace the weak link from the d^8 metal center.[44] The rearrangement is enthalpically driven by a desire to maximize the number of strong platinum-thioether bonds such that the more donating ligand becomes bidentate and the less donating ligand becomes monodentate.[31] Our initial hypothesis was that the formation of two homoligated complexes is driven by the maximization of solvation energy of each complex. This would result in PtCl$_2$(P,S-phenyl)$_2$ segregating to the less polar organic phase, while PtCl$_2$(P,S-ethyl-CONMe$_2$)$_2$ $[\mathbf{1}]^{2+}(\mathrm{Cl}^-)_2$ partitions into the aqueous phase.

To test this hypothesis, the heteroligated complex PtCl$_2$(P,S-Me)(P,S-phenyl-CONMe$_2$) $[\mathbf{5}]^{2+}(\mathrm{Cl}^-)_2$ was placed in a biphasic system. If the ligand rearrangement is driven by the solvation of polar moieties, the homoligated, fully closed complex PtCl$_2$(P,S-phenyl-CONMe$_2$)$_2$ should emerge over time in the D$_2$O layer. To our surprise, both ^{31}P{^{1}H} NMR spectroscopy (Figure 6b) and MALDI-TOF MS (Figure S45) revealed that the fully closed PtCl$_2$(P,S-Me)$_2$ (red dot) was the major species (δ_p 47.14, $^1J_{\mathrm{P-Pt}}$ = 3024 Hz) in the D$_2$O layer, while the fully closed PtCl$_2$(P,S-phenyl-CONMe$_2$)$_2$ was a minor species (δ_p 46.05; blue dot). The identity of the minor species was confirmed by its matching chemical shift with the independently synthesized and purified PtCl$_2$(P,S-phenyl-CONMe$_2$)$_2$ (δ_p 46.07; Figure S13). When given the choice, the less polar PtCl$_2$(P,S-Me)$_2$ selectively partitions into water and adopts the fully closed structural state, while the more water-soluble PtCl$_2$(P,S-phenyl-CONMe$_2$)$_2$ partitions into DCM. These results suggest that the ligand rearrangement observed in a biphasic medium stems from the driving force to maximize the number of stronger platinum-thioether bonds (i.e., in the case of complex $[\mathbf{5}]^{2+}$, those of P,S-Me). The relative polarity of the P,S-ligands plays only a minor role in determining the extent of rearrangement. Compared to $[\mathbf{5}]^{2+}(\mathrm{Cl}^-)_2$, a faster and more complete rearrangement is observed for $[\mathbf{3}]^{2+}(\mathrm{Cl}^-)_2$, as only the later possesses ligands whose polarity and donor strength differences work in tandem. Similar ligand sorting also occurs for PtCl$_2$(P,S-ethyl-CONMe$_2$)(P,S-phenyl-CONMe$_2$) $[\mathbf{4}]^{2+}(\mathrm{Cl}^-)_2$ in the D$_2$O/CD$_2$Cl$_2$ biphasic medium (Figure S35). Crucially, ligand sorting did not occur when chlorides were abstracted from the complexes using two equivalents of silver nitrate prior to phase transfer (Figure S36), confirming that the rearrangement proceeds via a HILR-type mechanism.

Biphasic Rearrangement of Heteroligated Complexes in the Presence of Large Counteranions. Inspired by the selective phase transfer from a mixture of homoligated complexes, we hypothesized that iodide would facilitate the rearrangement of heteroligated complexes by partitioning and stabilizing one of the two homoligated complexes into the less polar organic phase. To test this hypothesis, we added sodium iodide to the heteroligated, fully closed complex $[\mathbf{3}]^{2+}(\mathrm{Cl}^-)_2$ (Figure 7a) in a CD$_2$Cl$_2$/D$_2$O biphasic medium. The aqueous phase was acidified to prevent undesirable degradation in prolonged experiments (Figure S37). Upon the addition of one equivalent of NaI to complex $[\mathbf{3}]^{2+}(\mathrm{Cl}^-)_2$, the ^{31}P{^{1}H} NMR spectrum (Figure 7b) revealed the emergence of the fully closed homoligated complex Pt(P,S-ethyl-CONMe$_2$)$_2{}^{2+}$ $[\mathbf{1}]^{2+}$ (δ_p 46.56, $^1J_{\mathrm{P-Pt}}$ = 3062 Hz) in the D$_2$O layer within one day, along with the complete disappearance of the two downfield doublets (insert, Figure 6b) that correspond to the heteroligated, fully closed complex $[\mathbf{3}]^{2+}$. The broad ^{31}P{^{1}H} signals (δ_p 46.73, $^1J_{\mathrm{P-Pt}}$ = 3424 Hz; δ_p 3.72, $^1J_{\mathrm{P-Pt}}$ = 3099 Hz) in the CD$_2$Cl$_2$ layer suggests that both hemilabile ligands (P,S-ethyl-CONMe$_2$ and P,S-phenyl) were present, undergoing "windshield wiper" motion as well as rapid ligand exchange with one another.[30,33] The presence of [PtI(P,S-phenyl)$_2$]$^+$ (major species) and [PtI(P,S-ethyl-CONMe$_2$)(P,S-phenyl)]$^+$ (minor species) were confirmed by MALDI-TOF MS (Figure S48). We speculated that, if a second equivalent of NaI was added, both homoligated complexes would fully partition into

DCM and rearrange to reform the heteroligated, semi-open complex [**3**-I]$^+$ with an iodide counteranion. After adding a second equivalent of NaI and stirring the mixture for 1 day, the $^{31}P\{^1H\}$ NMR spectrum (Figure 7b) revealed that the $^{31}P\{^1H\}$ signal in the D_2O layer disappeared while a sharp downfield (δ_P 48.06, $^1J_{P-Pt}$ = 3361 Hz, $^3J_{P-P}$ = 12.1 Hz) and upfield doublet (δ_P 2.09, $^1J_{P-Pt}$ = 3078 Hz, $^3J_{P-P}$ = 12.7 Hz) emerged in DCM, indicating the formation of a heteroligated, semi-open complex. The distinct chemical shifts are characteristic of an inner sphere iodide,[41] and MALDI-TOF MS characterization confirmed its identity as [**3**-I]$^+$ (Figure S49).

Finally, the sequential addition of PPN$^+$Cl$^-$ and NaI enables a reversible sorting of the hemilabile ligands, switching between two supramolecular ensembles: the phase-separated complexes and the DCM-bound heteroligated complex (Figure 7a). After the addition of one equivalent of PPN$^+$Cl$^-$, the $^{31}P\{^1H\}$ signal (δ_P 46.56, $^1J_{P-Pt}$ = 3062 Hz) that corresponds to the fully closed [**1**]$^{2+}$ re-emerged in the D_2O layer (Figure 7b). This signifies that PPN$^+$Cl$^-$ substitutes one equivalent of I$^-$ with one equivalent of Cl$^-$ in the equilibrating mixture of metal complexes and hemilabile ligands, changing the system's thermodynamic landscape to favor the formation of phase-separated homoligated complexes. Heteroligated complex [**5**]$^{2+}$(Cl$^-$)$_2$ was also subjected to the sequential addition of NaI and PPN$^+$Cl$^-$ in a biphasic medium, yielding identical sorting behavior (Figure S38). Under a biphasic medium, the addition of suitable counteranions can not only modulate the partitioning and structural state of WLA complexes but also restructure these dynamic architectures.

■ CONCLUSIONS

This work showcases the interdependent roles of charge, solubility, and coordination strength on determining WLA metal complex structure, especially in biphasic media. Taken together, the design considerations garnered from these studies enable one to deliberately and reversibly alter the ligand composition and conformation of WLA complexes via a combination of salt metathesis reactions and solvent media exchange. Looking forward, we envision that the dynamic character of WLA complexes being harnessed for effecting novel structural regulation processes, such as modulating the conformations of biopolymers in water and counterion-mediated uptake, transport, and release of guest molecules in biphasic media.

■ EXPERIMENTAL SECTION

Synthesis of Homoligated WLA Complexes. Tweezer complexes were assembled in high yields (see SI Section 1) by combining two equivalents of phosphino-thioether (P,S) ligands with one equivalent of dichloro(1,5-cyclooctadiene)platinum(II) ($PtCl_2$(cod)) in DCM under an inert atmosphere. All homoligated complexes were characterized in the solution state by multinuclear NMR spectroscopy (SI Section 2) and mass spectroscopy (SI Section 4).

Synthesis of Heteroligated WLA Complexes. In a typical heteroligated complex, the two ligands should possess thioethers with sufficiently different donor strengths (e.g., alkyl vs aryl thioethers) to prevent scrambling.[30,31,41] Heteroligated complexes were assembled in a stepwise fashion. One equivalent of the first P,S ligand was mixed with one equivalent of $PtCl_2$(cod) in DCM in an inert atmosphere to give a monoligated complex, which was then combined with one equivalent of the second P,S ligand to give a heteroligated complex. All complexes were characterized by multinuclear NMR spectroscopy (SI Section 2) and mass spectroscopy (SI Section 4).

Phase Transfer Experiments. A 10 mL vial was loaded with the complex of interest, CD_2Cl_2 (0.7 mL), and D_2O (0.7 mL). The mixture was allowed to stir and equilibrate at room temperature for the specified period of time. The salt of interest (e.g., PPN$^+$Cl$^-$) was dissolved in CD_2Cl_2 or D_2O, added to the vial, and stirred. Each phase was carefully pipetted and transferred to separate NMR tubes for characterization. Specific reaction conditions can be found in the SI Table S2.

Multinuclear NMR Spectroscopy. Deuterated solvents (CD_2Cl_2 and D_2O) were purchased from Cambridge Isotope Laboratories and used as received. Multinuclear ($^{31}P\{^1H\}$, $^{13}C\{^1H\}$, and ^1H) NMR spectra were obtained when applicable. ^1H, $^{13}C\{^1H\}$, $^{31}P\{^1H\}$, and ^{31}P NMR spectra were recorded on a Bruker Avance 400 MHz NMR spectrometer at 298 K, and chemical shifts (δ) are given in parts per million. ^1H NMR spectra were referenced to residual proton resonances in the deuterated solvents (dichloromethane-d_2 = δ 5.32; deuterium oxide = δ 4.90), while absolute referencing was applied for heteronuclear NMR spectra (Ξ_C = 25.145020; Ξ_P = 40.480742).

The $^{31}P\{^1H\}$ NMR spectra of homoligated complexes in the fully closed state show a downfield singlet (~45 ppm in D_2O), with flanking satellites due to $^{31}P-^{195}Pt$ coupling, while that of a closed, heteroligated complex shows two downfield doublets due to coupling between two inequivalent ^{31}P nuclei. The $^{31}P\{^1H\}$ NMR spectra of heteroligated complexes in the semi-open state typically show a downfield doublet at ~45 ppm, corresponding to the "closed" phosphino-thioether ligand and an upfield doublet at ~8 ppm, originating from the "open" phosphino-thioether ligand.

High-Resolution Mass Spectroscopy. High resolution mass spectra (HRMS) were recorded on an Agilent 6120 LC-TOF instrument in positive ion mode. Matrix-assisted ionization desorption ionization-time-of-flight mass spectra (MALDI-TOF MS) were recorded on an AutoFlex-III (Bruker) in positive ion or negative ion mode, and the samples were prepared with the matrix 2,5-dihydroxybenzoic acid.

SCXRD Studies. Crystals of suitable size and quality were chosen and mounted on a MITIGEN holder or a mylar loop with Paratone oil on a Bruker APEX-II CCD diffractometer with Mo Kα radiation ([**1**]$^{2+}$(SCN$^-$)$_2$), a Rigaku XtaLAB Synergy R, DW system, HyPix diffractometer with Cu Kα radiation ([**2**] and [**5**-Cl]$^+$Cl$^-$), or a Rigaku XtaLAB Synergy, single source at offset/far, HyPix diffractometer with Mo Kα radiation ([**1**-2CN] and $PtCl_2$(P,S-phenyl-NH_2)$_2$). The crystals were kept at 100 to 120 K during data collection. With the exception of [**5**-Cl]$^+$Cl$^-$, the structures were solved using Olex2[45] with the ShelXT structure solution program[46] using Intrinsic Phasing and refined with the ShelXL refinement package using Least Squares minimization.[47] The structure of [**5**-Cl]$^+$Cl$^-$ was solved instead with the XS structure solution program[48] using the Patterson Method. Solvent masking was implemented in Olex2 for the structure Pt(P,S-ethyl-SO_3)$_2$ [**2**]·H_2O to remove the solvent molecules' electronic contribution from the refinement. As the exact solvent composition in the crystal is not known, only the atoms used in the refinement model are reported in the formula here.

■ ASSOCIATED CONTENT

Supporting Information

The Supporting Information is available free of charge at https://pubs.acs.org/doi/10.1021/acs.inorgchem.0c03708.

Synthetic procedures and spectral data (PDF)

Accession Codes

CCDC 2047632−2047636 contain the supplementary crystallographic data for this paper. These data can be obtained free of charge via www.ccdc.cam.ac.uk/data_request/cif, or by emailing data_request@ccdc.cam.ac.uk, or by contacting The Cambridge Crystallographic Data Centre, 12 Union Road, Cambridge CB2 1EZ, UK; fax: +44 1223 336033.

AUTHOR INFORMATION

Corresponding Author

Chad A. Mirkin − *Department of Chemistry and International Institute for Nanotechnology, Northwestern University, Evanston, Illinois 60208-3113, United States;* orcid.org/0000-0002-6634-7627; Email: chadnano@northwestern.edu

Authors

Ho Fung Cheng − *Department of Chemistry and International Institute for Nanotechnology, Northwestern University, Evanston, Illinois 60208-3113, United States;* orcid.org/0000-0003-2580-0912

McKinley K. Paul − *Department of Chemistry and International Institute for Nanotechnology, Northwestern University, Evanston, Illinois 60208-3113, United States;* orcid.org/0000-0002-3929-1883

Andrea I. d'Aquino − *Department of Chemistry and International Institute for Nanotechnology, Northwestern University, Evanston, Illinois 60208-3113, United States;* orcid.org/0000-0002-4204-8219

Charlotte L. Stern − *Department of Chemistry and International Institute for Nanotechnology, Northwestern University, Evanston, Illinois 60208-3113, United States;* orcid.org/0000-0002-9491-289X

Complete contact information is available at:
https://pubs.acs.org/10.1021/acs.inorgchem.0c03708

Author Contributions

‡H.F.C. and M.K.P. contributed equally.

Notes

The authors declare no competing financial interest.

ACKNOWLEDGMENTS

This material is based upon work supported by the National Science Foundation under Grant CHE-1709888 and the Sherman Fairchild Foundation, Inc. This work also made use of instruments of IMSERC at Northwestern University that have received support from the Soft and Hybrid Nanotechnology Experimental (SHyNE) Resource (NSF ECCS-1542205), the State of Illinois, and International Institute for Nanotechnology (IIN). A.I.d. acknowledges a National Science Foundation Graduate Research Fellowship.

ABBREVIATIONS

HILR, halide-induced ligand rearrangement; MALDI-TOF MS, matrix-assisted laser desorption ionization-time-of-flight mass spectroscopy; NMR, nuclear magnetic resonance spectroscopy; P,S, phosphino-thioether; WLA, weak-link approach

REFERENCES

(1) Sheldon, R. A. Green solvents for sustainable organic synthesis: state of the art. *Green Chem.* **2005**, *7*, 267−278.

(2) Chu, Q.; Yu, M. S.; Curran, D. P. New fluorous/organic biphasic systems achieved by solvent tuning. *Tetrahedron* **2007**, *63*, 9890−9895.

(3) Shukla, S. K.; Pandey, S.; Pandey, S. Applications of ionic liquids in biphasic separation: Aqueous biphasic systems and liquid-liquid equilibria. *J. Chromatogr. A* **2018**, *1559*, 44−61.

(4) Grommet, A. B.; Nitschke, J. R. Directed Phase Transfer of an FeII4L4 Cage and Encapsulated Cargo. *J. Am. Chem. Soc.* **2017**, *139*, 2176−2179.

(5) Zhang, D.; Ronson, T. K.; Mosquera, J.; Martinez, A.; Nitschke, J. R. Selective Anion Extraction and Recovery Using a FeII4L4 Cage. *Angew. Chem., Int. Ed.* **2018**, *57*, 3717−3721.

(6) Nguyen, B.-N. T.; Grommet, A. B.; Tron, A.; Georges, M. C. A.; Nitschke, J. R. Heat Engine Drives Transport of an FeII4L4 Cage and Cargo. *Adv. Mater.* **2020**, *32*, 1907241.

(7) Zhang, D.; Ronson, T. K.; Lavendomme, R.; Nitschke, J. R. Selective Separation of Polyaromatic Hydrocarbons by Phase Transfer of Coordination Cages. *J. Am. Chem. Soc.* **2019**, *141*, 18949−18953.

(8) Yoshizawa, M.; Tamura, M.; Fujita, M. Chirality enrichment through the heterorecognition of enantiomers in an achiral coordination host. *Angew. Chem., Int. Ed.* **2007**, *46*, 3874−3876.

(9) Grancha, T.; Carne-Sanchez, A.; Hernandez-Lopez, L.; Albalad, J.; Imaz, I.; Juanhuix, J.; Maspoch, D. Phase Transfer of Rhodium(II)-Based Metal-Organic Polyhedra Bearing Coordinatively Bound Cargo Enables Molecular Separation. *J. Am. Chem. Soc.* **2019**, *141*, 18349−18355.

(10) Horvath, I. T.; Rabai, J. Facile catalyst separation without water: fluorous biphase hydroformylation of olefins. *Science* **1994**, *266*, 72−75.

(11) Sheldon, R. Catalytic reactions in ionic liquids. *Chem. Commun.* **2001**, 2399−2407.

(12) Dupont, J.; de Souza, R. F.; Suarez, P. A. Z. Ionic Liquid (Molten Salt) Phase Organometallic Catalysis. *Chem. Rev.* **2002**, *102*, 3667−3691.

(13) Starks, C. M. Phase-transfer catalysis. I. Heterogeneous reactions involving anion transfer by quaternary ammonium and phosphonium salts. *J. Am. Chem. Soc.* **1971**, *93*, 195−199.

(14) Albanese, D. Liquid-liquid phase transfer catalysis: basic principles and synthetic applications. *Catal. Rev.: Sci. Eng.* **2003**, *45*, 369−395.

(15) Ooi, T.; Maruoka, K. Recent advances in asymmetric phase-transfer catalysis. *Angew. Chem., Int. Ed.* **2007**, *46*, 4222−4266.

(16) Ito, H.; Kusukawa, T.; Fujita, M. Wacker oxidation in an aqueous phase through the reverse phase-transfer catalysis of a self-assembled nanocage. *Chem. Lett.* **2000**, *29*, 598−599.

(17) Reetz, M. T.; Waldvogel, S. R. β-Cyclodextrin-modified diphosphines as ligands for supramolecular rhodium catalysts. *Angew. Chem., Int. Ed. Engl.* **1997**, *36*, 865−867.

(18) Bricout, H.; Hapiot, F.; Ponchel, A.; Tilloy, S.; Monflier, E. Chemically modified cyclodextrins: An attractive class of supramolecular hosts for the development of aqueous biphasic catalytic processes. *Sustainability* **2009**, *1*, 924−945.

(19) Shaughnessy, K. H. Hydrophilic Ligands and Their Application in Aqueous-Phase Metal-Catalyzed Reactions. *Chem. Rev.* **2009**, *109*, 643−710.

(20) McConnell, A. J.; Haynes, C. J. E.; Grommet, A. B.; Aitchison, C. M.; Guilleme, J.; Mikutis, S.; Nitschke, J. R. Orthogonal Stimuli Trigger Self-Assembly and Phase Transfer of FeII4L4 Cages and Cargoes. *J. Am. Chem. Soc.* **2018**, *140*, 16952−16956.

(21) Grommet, A. B.; Hoffman, J. B.; Percastegui, E. G.; Mosquera, J.; Howe, D. J.; Bolliger, J. L.; Nitschke, J. R. Anion Exchange Drives Reversible Phase Transfer of Coordination Cages and Their Cargoes. *J. Am. Chem. Soc.* **2018**, *140*, 14770−14776.

(22) Ding, Y.; Williams, N. H.; Hunter, C. A. A Synthetic Vesicle-to-Vesicle Communication System. *J. Am. Chem. Soc.* **2019**, *141*, 17847−17853.

(23) Farrell, J. R.; Mirkin, C. A.; Guzei, I. A.; Liable-Sands, L. M.; Rheingold, A. L. The weak-link approach to the synthesis of inorganic macrocycles. *Angew. Chem., Int. Ed.* **1998**, *37*, 465−467.

(24) Gianneschi, N. C.; Masar, M. S., III; Mirkin, C. A. Development of a Coordination Chemistry-Based Approach for Functional Supramolecular Structures. *Acc. Chem. Res.* **2005**, *38*, 825−837.

(25) Lifschitz, A. M.; Rosen, M. S.; McGuirk, C. M.; Mirkin, C. A. Allosteric Supramolecular Coordination Constructs. *J. Am. Chem. Soc.* **2015**, *137*, 7252−7261.

(26) Wiester, M. J.; Braunschweig, A. B.; Mirkin, C. A. Solvent and Temperature Induced Switching Between Structural Isomers of Rh(I)

Phosphinoalkyl Thioether (PS) Complexes. *Inorg. Chem.* **2010**, *49*, 7188−7196.

(27) Wiester, M. J.; Mirkin, C. A. Water-Soluble Macrocycles Synthesized via the Weak-Link Approach. *Inorg. Chem.* **2009**, *48*, 8054−8056.

(28) D'Aquino, A. I.; Cheng, H. F.; Barroso-Flores, J.; Kean, Z. S.; Mendez-Arroyo, J.; McGuirk, C. M.; Mirkin, C. A. An Allosterically Regulated, Four-State Macrocycle. *Inorg. Chem.* **2018**, *57*, 3568−3578.

(29) Anderson, G. K.; Kumar, R. Platinum(II) complexes of unsymmetrical, potentially bidentate ligands. *Inorg. Chem.* **1984**, *23*, 4064−4068.

(30) Rosen, M. S.; Spokoyny, A. M.; Machan, C. W.; Stern, C.; Sarjeant, A.; Mirkin, C. A. Chelating Effect as a Driving Force for the Selective Formation of Heteroligated Pt(II) Complexes with Bidentate Phosphino-Chalcoether Ligands. *Inorg. Chem.* **2011**, *50*, 1411−1419.

(31) Kennedy, R. D.; Machan, C. W.; McGuirk, C. M.; Rosen, M. S.; Stern, C. L.; Sarjeant, A. A.; Mirkin, C. A. General Strategy for the Synthesis of Rigid Weak-Link Approach Platinum(II) Complexes: Tweezers, Triple-Layer Complexes, and Macrocycles. *Inorg. Chem.* **2013**, *52*, 5876−5888.

(32) Roobottom, H. K.; Jenkins, H. D. B.; Passmore, J.; Glasser, L. Thermochemical radii of complex ions. *J. Chem. Educ.* **1999**, *76*, 1570−1573.

(33) Spokoyny, A. M.; Machan, C. W.; Clingerman, D. J.; Rosen, M. S.; Wiester, M. J.; Kennedy, R. D.; Stern, C. L.; Sarjeant, A. A.; Mirkin, C. A. A coordination chemistry dichotomy for icosahedral carborane-based ligands. *Nat. Chem.* **2011**, *3*, 590−596.

(34) Eisenberg, A. H.; Dixon, F. M.; Mirkin, C. A.; Stern, C. L.; Incarvito, C. D.; Rheingold, A. L. Binuclear Palladium Macrocycles Synthesized via the Weak-Link Approach. *Organometallics* **2001**, *20*, 2052−2058.

(35) Pringle, P. G.; Shaw, B. L. Heterobimetallic complexes via η^1-Ph2PCH2PPh2 complexes of platinum or palladium dicyanides. *J. Chem. Soc., Chem. Commun.* **1982**, 956−957.

(36) Eisenberg, A. H.; Ovchinnikov, M. V.; Mirkin, C. A. Stepwise Formation of Heterobimetallic Macrocycles Synthesized via the Weak-Link Approach. *J. Am. Chem. Soc.* **2003**, *125*, 2836−2837.

(37) Mendez-Arroyo, J.; Barroso-Flores, J.; Lifschitz, A. M.; Sarjeant, A. A.; Stern, C. L.; Mirkin, C. A. A Multi-State, Allosterically-Regulated Molecular Receptor With Switchable Selectivity. *J. Am. Chem. Soc.* **2014**, *136*, 10340−10348.

(38) McGuirk, C. M.; Mendez-Arroyo, J.; Lifschitz, A. M.; Mirkin, C. A. Allosteric Regulation of Supramolecular Oligomerization and Catalytic Activity via Coordination-Based Control of Competitive Hydrogen-Bonding Events. *J. Am. Chem. Soc.* **2014**, *136*, 16594−16601.

(39) Yoon, H. J.; Kuwabara, J.; Kim, J. H.; Mirkin, C. A. Allosteric Supramolecular Triple-Layer Catalysts. *Science* **2010**, *330*, 66−69.

(40) Lifschitz, A. M.; Young, R. M.; Mendez-Arroyo, J.; Stern, C. L.; McGuirk, C. M.; Wasielewski, M. R.; Mirkin, C. A. An allosteric photoredox catalyst inspired by photosynthetic machinery. *Nat. Commun.* **2015**, *6*, 6541.

(41) Ulmann, P. A.; Brown, A. M.; Ovchinnikov, M. V.; Mirkin, C. A.; DiPasquale, A. G.; Rheingold, A. L. Spontaneous formation of heteroligated PtII complexes with chelating hemilabile ligands. *Chem. - Eur. J.* **2007**, *13*, 4529−4534.

(42) Ulmann, P. A.; Mirkin, C. A.; Di Pasquale, A. G.; Liable-Sands, L. M.; Rheingold, A. L. Reversible Ligand Pairing and Sorting Processes Leading to Heteroligated Palladium(II) Complexes with Hemilabile Ligands. *Organometallics* **2009**, *28*, 1068−1074.

(43) Brown, A. M.; Ovchinnikov, M. V.; Mirkin, C. A. Heteroligated Rh(I) tweezer complexes. *Angew. Chem., Int. Ed.* **2005**, *44*, 4207−4209.

(44) Brown, A. M.; Ovchinnikov, M. V.; Stern, C. L.; Mirkin, C. A. Halide-induced supramolecular ligand rearrangement. *J. Am. Chem. Soc.* **2004**, *126*, 14316−14317.

(45) Dolomanov, O. V.; Bourhis, L. J.; Gildea, R. J.; Howard, J. A. K.; Puschmann, H. OLEX2: a complete structure solution, refinement and analysis program. *J. Appl. Crystallogr.* **2009**, *42*, 339−341.

(46) Sheldrick, G. M. SHELXT - Integrated space-group and crystal-structure determination. *Acta Crystallogr., Sect. A: Found. Adv.* **2015**, *71*, 3−8.

(47) Sheldrick, G. M. Crystal structure refinement with SHELXL. *Acta Crystallogr., Sect. C: Struct. Chem.* **2015**, *71*, 3−8.

(48) Sheldrick, G. M. A short history of SHELX. *Acta Crystallogr., Sect. A: Found. Crystallogr.* **2008**, *64*, 112−122.